NiCoCrAlYHf COATING EVOLUTION THROUGH MULTIPLE REFURBISHMENT PROCESSING ON A SINGLE CRYSTAL NICKEL SUPERALLOY

A Rowe
RWE npower, Whitehill Way, Swindon, Wiltshire, SN5 6PB
Department of Materials, Loughborough University, Loughborough, LE11 3TU, UK

M Karunaratne and R C Thomson
Department of Materials, Loughborough University, Loughborough, LE11 3TU, UK

ABSTRACT
A combination of creep tests, ex-service blade samples, thermodynamic equilibrium calculations, combined thermodynamic and kinetic calculations, image analysis, chemical composition mapping and heat treatments have been conducted on PWA1483 to determine if microstructural rejuvenation can be achieved when taking the presence of oxidation coatings into account as part of a blade refurbishment strategy.

The work has shown that the γ′ morphology changes during creep testing, and that through subsequent heat treatments the γ′ microstructure can be altered to achieve a similar γ′ size and distribution to the original creep test starting condition. Thermodynamic equilibrium calculations have been shown to be helpful in determining the optimum temperatures to be used for the refurbishment heat treatments.

The interaction of oxidation resistant coatings with the alloy substrate and refurbishment process have been explored with both experimental measurements and coupled thermodynamic and kinetic calculations. The predictive nature of the coupled thermodynamic and kinetic calculations was evaluated against an ex-service blade sample which had undergone refurbishment and further ageing. In general there was good agreement between the experimental observations and model predictions, and the modelling indicated that there were limited differences expected as a result of two different refurbishment methodologies. However, on closer inspection, there were some discrepancies occurring near the interface location between the coating and the base alloy. This comparison with experimental data provided an opportunity to refine the compositional predictions as a result of both processing methodologies and longer term exposure. The improved model has also been used to consider multiple processing cycles on a sample, and to evaluate the coating degradation between component service intervals and the consequences of rejuvenation of the blade with repeated engine exposure. The results from the experimental work and modelling studies potentially offer an assessment tool when considering a component for refurbishment.

Keywords: Creep, Coating, Refurbishment, Gas Turbine

INTRODUCTION
Coated single crystal nickel superalloys feature in the hottest areas of industrial gas turbines. As a consequence they undergo microstructural degradation during service which ultimately results in both a reduction of creep properties for the base alloy and coating degradation. The aim of this work is to explore the possibility of applying a refurbishment heat treatment to rejuvenate the microstructure of the bulk alloy combined with reapplication of a coating system, which should enable reuse of the component and hence prolong its' service life. It is therefore necessary to develop techniques to rapidly quantify the microstructure of coated nickel superalloys to assess

the outcome of any refurbishment heat treatments, and also to make predictions of coating evolution with time at temperature. The single crystal nickel superalloy PWA1483 has been selected in this work to undergo mechanical and thermal degradation, followed by a subsequent rejuvenation process and the effect on the microstructure explored fully using a range of analytical techniques.

EXPERIMENTAL AND MODELLING METHODS

Experimental

Creep test pieces of diameter 5 mm and gauge length 25 mm were machined from samples of the as-received homogenised PWA1483 alloy and were subsequently coated with a 100 µm thick oxidation resistant coating (NiCoCrAlYHf) typical of those applied to industrial components. An ex-service single crystal blade of PWA1483 which had undergone ~27,000 hours of engine exposure was used as an additional source of test coupons for comparison purposes. Table 1 provides a summary of the nominal chemical compositions of the alloy, the coating used on the creep samples and the coating present on the ex-service blade (NiCoCrAlYRe). The coated samples were sprayed using high velocity oxyfuel with a commercially available NiCoCrAlYHf powder, followed by common post-coating heat treatments involving a high temperature diffusion treatment and a lower temperature ageing; this condition is subsequently referred to as 'as coated'. Constant load creep tests were performed at 950°C in air with a load calculated to give rupture at approximately 8000 hours. A selection of creep samples were interrupted after half life, i.e. 4000 hours, and the remainder were stopped after 8000 hours if rupture had not occurred. Microstructural evaluation was then carried out on as-received material, coated material, materials from interrupted and ruptured creep tests and the ex-service blade sample, with respect to both the bulk microstructure and the coating. The initial microstructural evaluation studies were carried out on prepared microsections, which had been lightly electrolytically etched with a mixture of 1% citric acid and 1% ammonium sulphate in distilled water to selectively dissolve the γ phase. These were subsequently examined in directions parallel to the [001] single crystal growth direction using scanning electron microscopy (SEM) in conjunction with an energy dispersive spectrometer (EDS).

Table 1. Nominal chemical composition in weight percent of the nickel based superalloys and oxidation coatings used.

Element	Al	Ti	Cr	Co	Mo	Hf	Ta	W	Re	Y	Zr	Ni
PWA1483	3.6	4.0	12.1	9.1	1.9	-	5.0	3.8	-	-	-	Bal
NiCoCrAlYHf	12.5	-	17	22	-	0.25	-	-	-	0.6	-	Bal
NiCoCrAlYRe	10.7	-	24.4	8.8	-	-	-	-	2.3	0.5	-	Bal

A subsequent heat treatment, based on thermodynamic calculations, was carried out on the PWA1483 crept samples to alter the γ′ structure, which were then also examined to quantify the changes to the γ′. The ex-service blade had the coating removed and received the same heat treatments as the creep samples. The ex-service blade was recoated with the same NiCoCrAlYHf powder as the creep samples but with a thickness of ~300µm and a thermal barrier coating (TBC) coating of ~200µm. The recoated blades samples were then thermally exposed for ~10,000 hours using similar thermal conditions and were examined to quantify changes in the NiCoCrAlYHf coating.

Thermodynamic and Kinetic Modelling

Thermodynamic equilibrium calculations have been performed using JMatPro 4.1 (Java-based Materials Properties software)[1] to determine a heat treatment window between the γ′ solvus and

the liquidus, in order to specify a possible rejuvenation heat treatment for γ′. The calculations used the nominal composition of the alloy, actual measured compositions of the base alloy and from the interdiffusion zone and slight theoretical changes to the composition as a function of possible segregation in the alloy to give a range of possible γ′ solvus temperatures and liquidus temperatures.

Coupled thermodynamic and kinetic calculations were undertaken to determine how the chemical composition varied between the coating and the substrate as a function of time and temperature of exposure. The initial calculations mimicked the thermal exposure of the creep and blade samples, with a further round of calculations undertaken incorporating experimentally measured compositions for additional predictions. The numerical model used for the calculations combined multicomponent diffusion with equilibrium thermodynamics and surface oxidation[2]. The diffusion calculation was based on finite-differences which took into account the phase composition and diffusion within phases by linking with MTDATA[3] and a database of thermodynamic parameters[4] whereas the surface oxidation of Al was simulated using a published model[5]. The calculations were performed on a parallel cluster, typically with 72 nodes and 504 grid points. The removal and re-deposition of coating layers were simulated numerically by interpolating concentration profiles using cubic splines.

RESULTS & DISCUSSION

γ′ Evolution

The shape and size of γ′ precipitates changes with applied temperature and stress and therefore when considering refurbishment of such an alloy system, it is important that the size differences are characterised and quantified to understand the effects of heat treatment.

The effects of heat treatment have been considered using the thermodynamic calculations to determine the temperature difference between the γ′ solvus and the liquidus. This has resulted in the prediction of a ‘temperature window’ within which it would be expected that the γ′ precipitates would be fully taken into solution before the onset of melting. This is shown graphically for PWA1483 in Figure 1, and Table 2 contains a summary of the results.

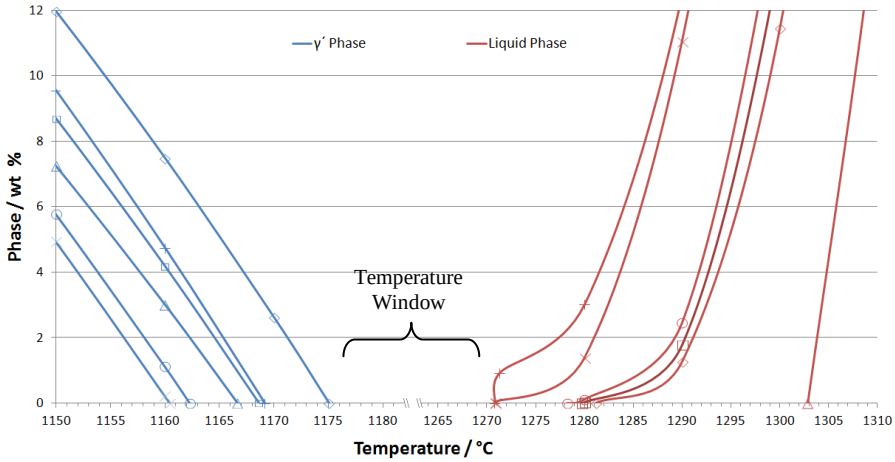

Figure 1. A summary plot of thermodynamic equilibrium calculations for γ′ solvus and liquidus temperatures for PWA1483, each symbol on a line represents a different composition variant.

The calculations show that there is a temperature window that can be used to fully solution the γ′ whilst trying to reduce the risk of any incipient melting. An appropriate temperature within the temperature window was subsequently used to rejuvenate the γ′ structure for the alloy.

Table 2 Summary of the highest γ′ solvus and lowest liquidus temperatures which have been calculated for PWA1483.

Alloy	γ′ Solvus / °C	Liquidus / °C	Difference / °C
PWA1483	1175	1270	95

The γ′ size was characterised using image analysis from SEM images to determine a γ′ thickness/diameter if cubic/spherical and in the case that the γ′ had elongated to form rafts, the raft thickness was determined: all of these dimensions are referred to as a 'width'. The specific details on the methodology used to characterise these microstructural forms have been detailed elsewhere[6].

The PWA1483 γ′ microstructure evolved during creep testing and Figure 2 shows how the γ′ structure changes during creep testing. There is a clear change from cubic γ′ to an elongated, or rafted, microstructure.

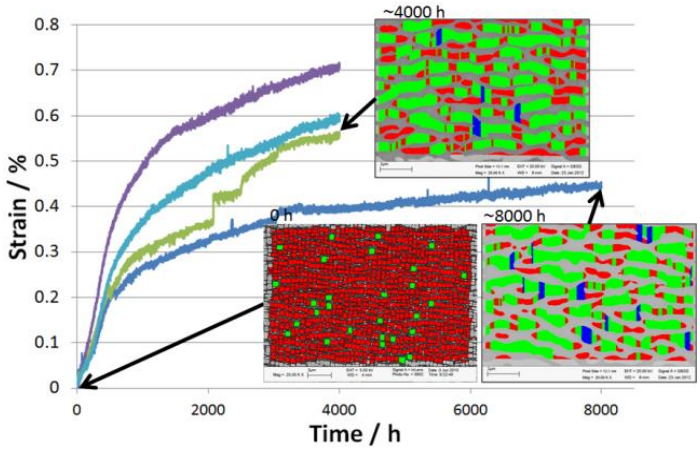

Figure 2. Strain against time plot for the coated creep test conducted at 950°C with inlays of γ′ morphology at different times during the creep test for PWA1483 at 125 MPa, The direction of the applied stress to the inlays of the γ′ morphology is top to bottom for all images which are at the same magnification. Classification of the γ′ width: Red: 0-0.5 µm, Green: 0.5-1.0 µm, Blue: 1.0-1.5 µm; Yellow: 1.5-2.0 µm, Cyan >2.0 µm.

The rafted microstructure from the creep samples had a heat treatment which was within the temperature window expected to rejuvenate the γ′ microstructure. Figure 3 i) shows the as coated microstructure and Figure 3 ii) shows that for an 8000 h creep sample which originally had a rafted microstructure it is possible to fully re-solution the alloy to form a more cubic γ′ microstructure. Figure 4 shows a histogram distribution for the γ′ microstructure width measurements from the samples which had received different heat treatments and creep testing. The γ′ distribution obtained from the fully re-solutioned sample is observed to be similar to the γ′ distribution of the as-coated sample. The images presented in Figures 3 i) and ii), show that the γ′

structure after full re-solution does not quite have the same regular cubic appearance as the as-coated microstructure. The subsequent creep testing for the fully re-solutioned samples should indicate if there has been a significant change to the creep properties of the alloy.

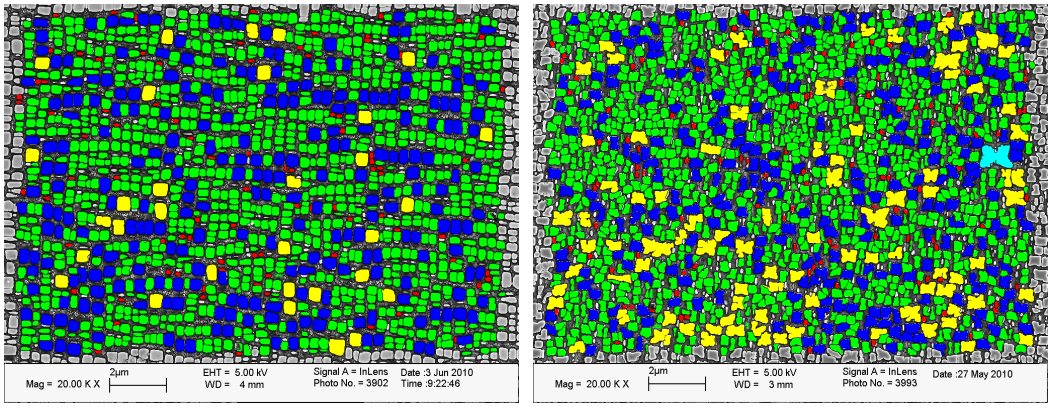

i) ii)

Figure 3. Secondary electron SEM images taken from alloy PWA1483 shows the γ' appearance in the dendrite core for i) after coating and aging heat treatments(0 h) ii) γ' appearance after high temperature heat treatment and subsequent cooling for full re-solution of γ'. The images have been processed to identify individual particles with the different colours indicating particle width. Classification of the γ' particle width: Red: 0-0.2 µm, Green: 0.2-0.4 µm, Blue: 0.4-0.5 µm; Yellow: 0.5-1.0 µm, Cyan >1.0 µm.

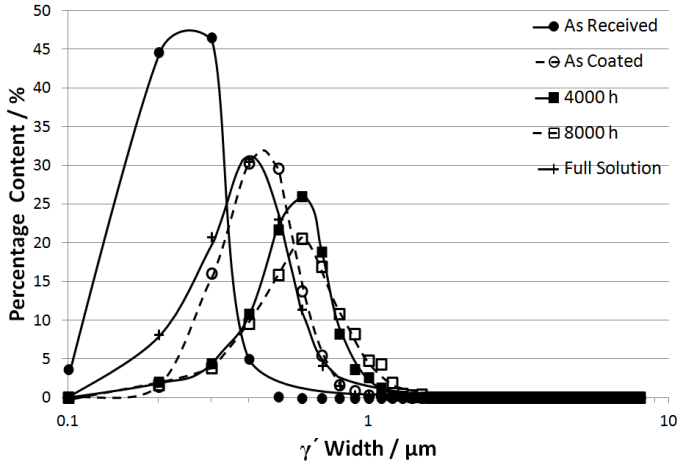

Figure 4. Histogram distribution plot for γ´ width at different points during the PWA1483 creep sample life from original homogenised casting, coating, creep exposure and a full solution heat treatment after creep exposure.

Coating Evolution

Creep Samples

The oxidation coating on the creep samples has been examined using EDS to determine how the chemical composition and coating phases have changed during creep exposure. These measured compositions and phases have then been compared to the predictions of the coupled thermodynamic and kinetic calculations.

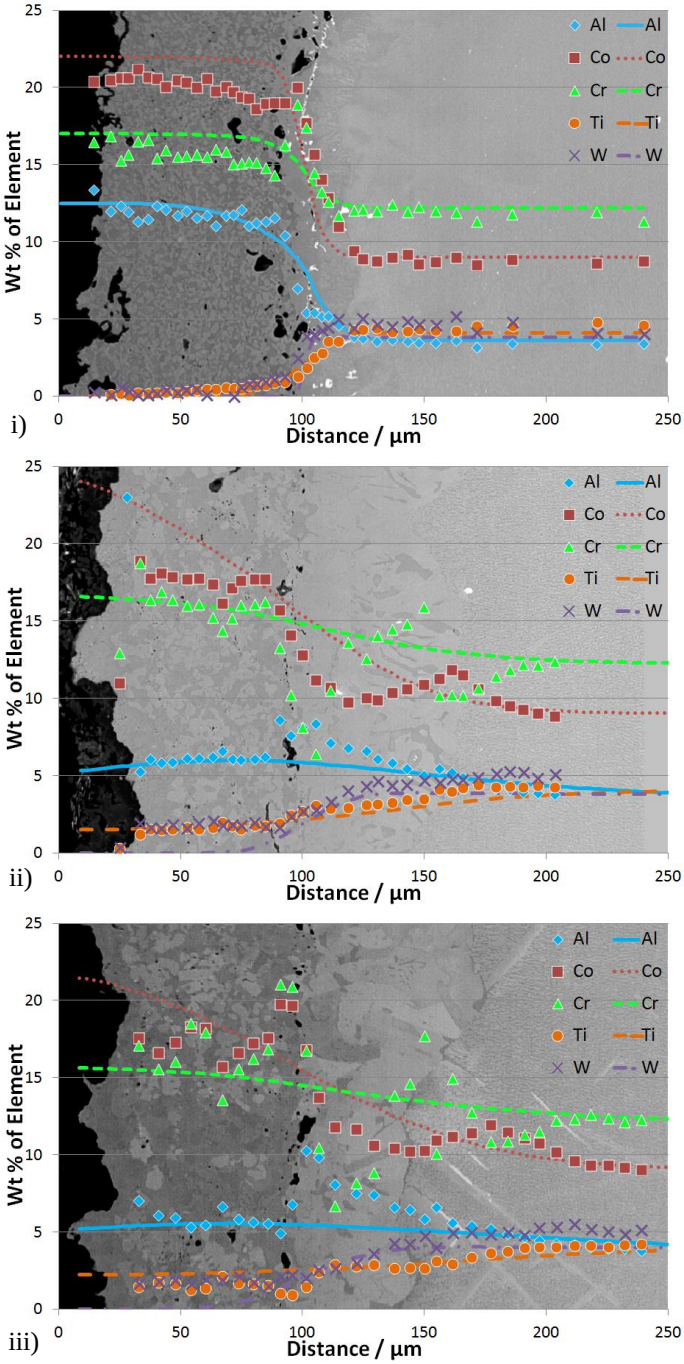

Figure 5. A series of plots for PWA1483 i) as coated, ii) 4000 hours of creep exposure and iii) 8000 hours of creep exposure showing how the elemental concentrations of Al, Co, Cr, Ti, and W vary as function of position. The points are from measurements taken using EDS in an SEM and the lines on the plots are the predictions from the combined thermodynamic and kinetic calculations. The ~100µm position represents the original coating/alloy interface. The data are overlaid on a corresponding SEM backscattered detector image.

Figure 5 shows how the composition of the coating and interface changes with thermal/creep exposure together with the corresponding SEM image. It can be seen that original Al content of around 12.5 wt.% has decreased significantly to around 5 wt.%; the thermodynamic and kinetic calculations also identify this change. The thermodynamic and kinetic calculations indicate that the beta phase in the coating after 4000 hours has been transformed to γ′. Indeed, no significant levels of beta phase were found by measurement for the 4000 and 8000 hours creep samples, which was consistent with the coupled thermodynamic and kinetic calculations. SEM examination of the original coating showed that beta occupied an area of ~45%, as shown in Figure 6, which can be assumed to correspond to ~45 wt.% beta. The thermodynamic and kinetic calculations indicate the starting beta proportion would have been ~52 wt%, and given that this figure excludes the porosity present in the coating, there is a reasonable correlation between the predicted and observed amounts.

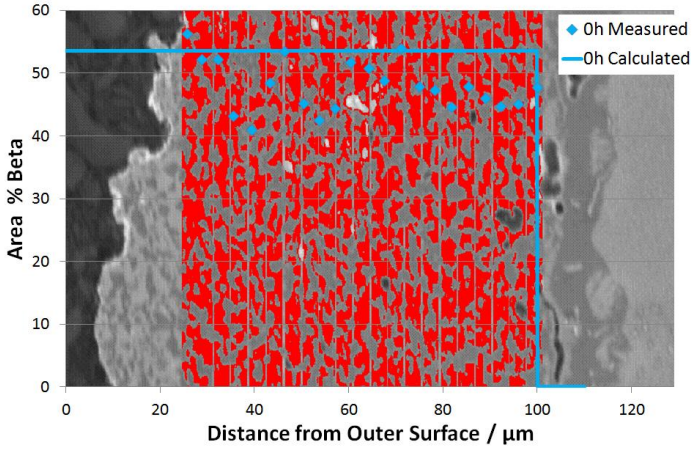

Figure 6. A plot showing how the beta phase varies through the as coated creep sample. The points are from measurement and the lines are from coupled thermodynamic and kinetic calculations. The data are overlaid on a corresponding SEM image with red indicating the phase being analysed.

The measured Cr concentration in the creep sample was observed to be different from the thermodynamic and kinetic calculations in the interface region. However, the model prediction is for the mean Cr level, whereas it was observed that the points at which the Cr levels were measured, when overlaid on the back scattered electron SEM image, aligned with particular microstructural features and in particular with Cr-rich precipitates.

The coupled thermodynamic and kinetic calculations then used both the predicted and measured compositions after 4000 hours to simulate what would occur during refurbishment and repeated thermal/creep exposure. The results in Figures 7 are for the predicted composition after 4000 hours, whereas Figure 8 uses the measured composition after 4000 hours as the starting reference for the subsequent calculations to determine the likely effect of the refurbishment process. The results shown in Figures 7 and 8 are for two refurbishment conditions considering scenarios when both 100 µm and 120 µm of material has been removed. There are only limited differences observed between the two data sets after repeated 4000 hours of thermal exposure at 950°C. This may suggest that the amount of material taken from the base metal has little impact on the coating behaviour in the long term. This was also the case where the 100 µm of material removal

intersected the Cr depleted region from Figure 5 ii), because after the full re-solution the Cr level has appeared to have redistributed, as shown in Figure 8 i). This will need to be confirmed with measurement taken from processed creep samples in the future.

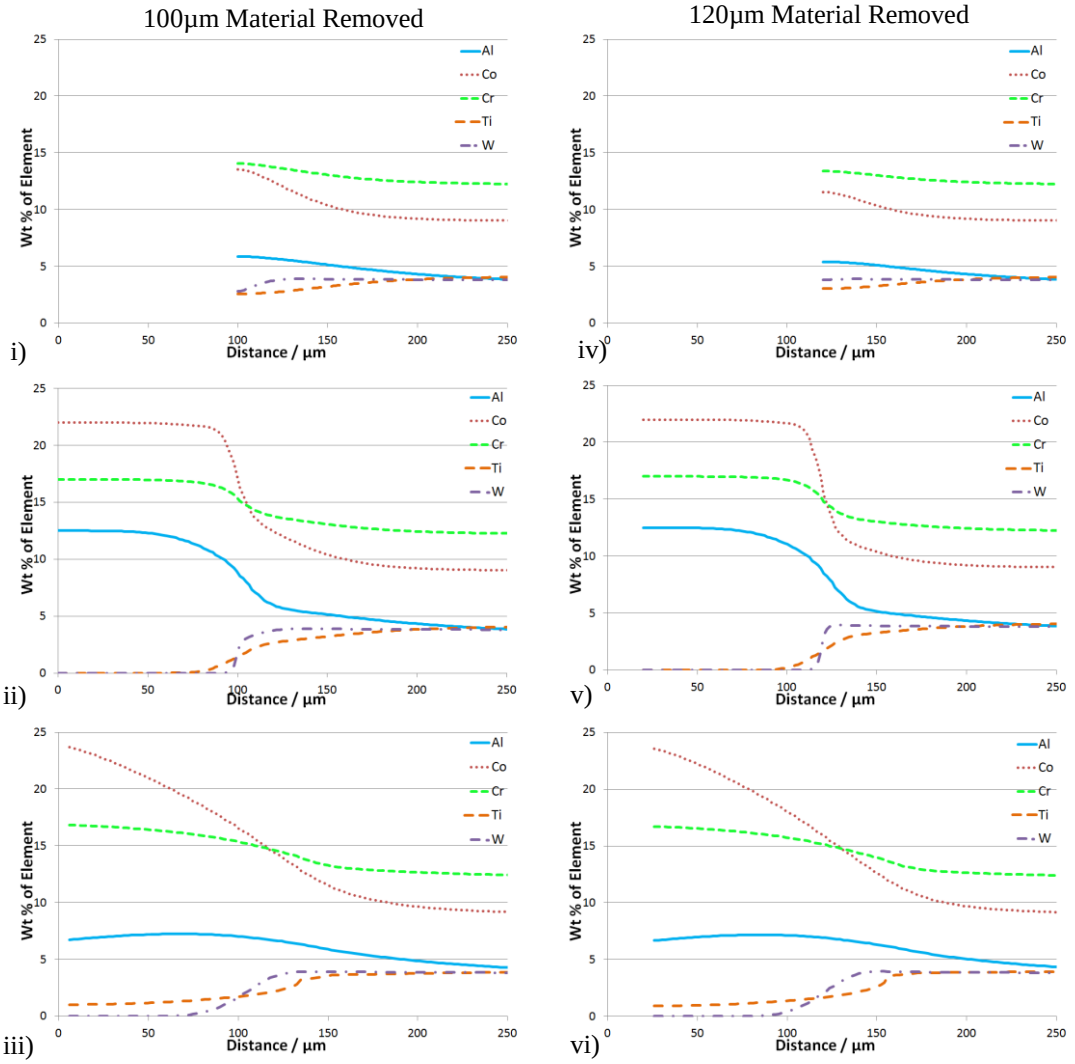

Figure 7. A series of combined thermodynamic and kinetic calculations plots for the calculated composition of the PWA1483 4000 hour creep sample i) after 100µm material removal and full γ′ solution ii) after coating diffusion and age, iii) after 4000 hours of thermal exposure at 950°C, iv) after 120µm material removed and full γ′ solution v) after coating diffusion and age and vi) after 4000 hours of thermal exposure at 950°C.

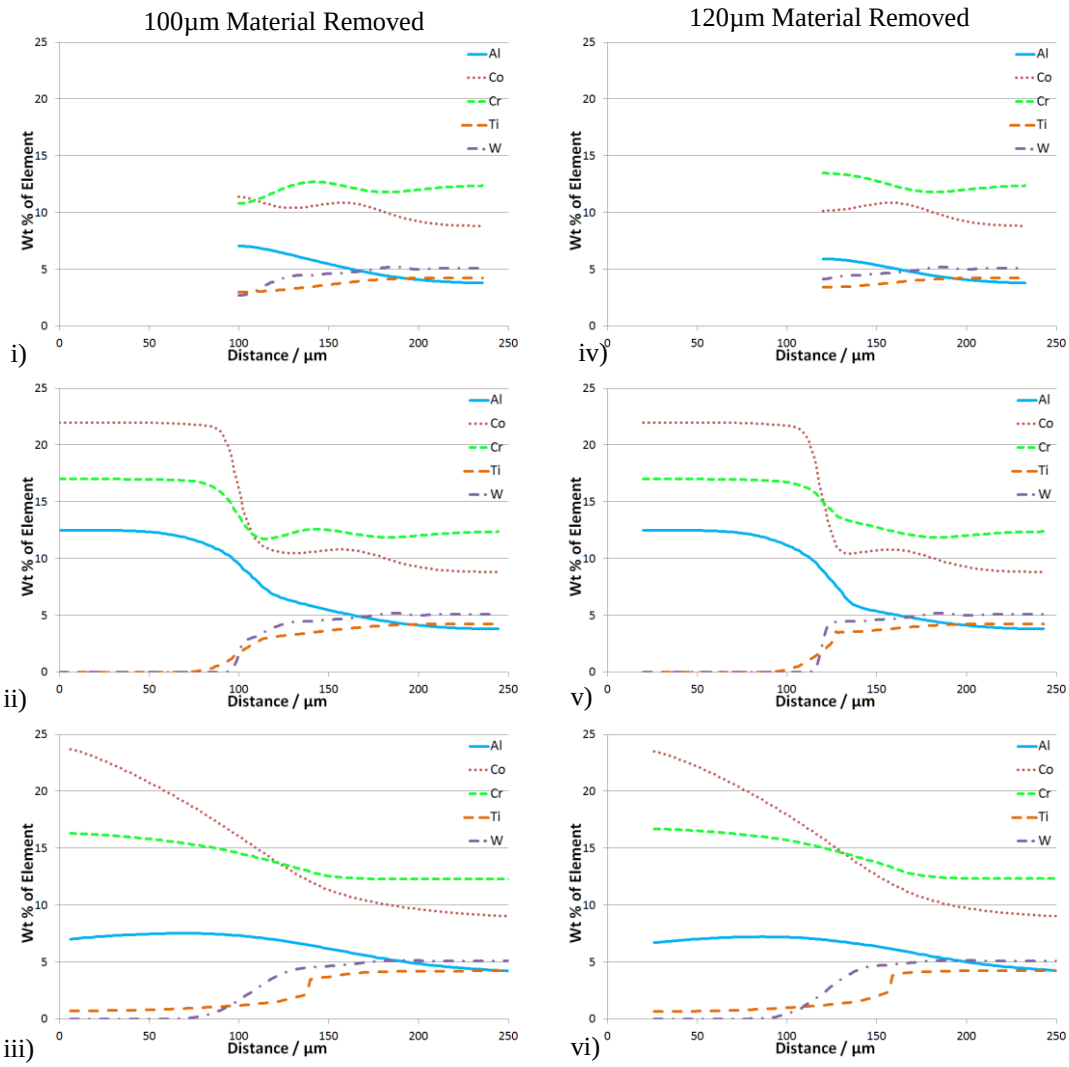

Figure 8. A series of combined thermodynamic and kinetic calculations plots for the measured composition in the PWA1483 4000 hour creep sample i) after 100µm material removal and full γ′ solution ii) after coating diffusion and age, iii) after 4000 hours of thermal exposure at 950°C, iv) after 120µm material removed and full γ′ solution v) after coating diffusion and age and vi) after 4000 hours of thermal exposure at 950°C.

Blade Samples

In order to compare the crept samples, with an ex-service blade, the original NiCoCrAlYRe blade coating which was ~150µm thick was removed and the blade samples were then given the same heat treatment as the creep samples for the base alloy in order to re-solution the γ′. The NiCoCrAlYHf coating, which was the same as that used for the creep samples, was applied to the blade samples to a thickness ~300 µm; the last ~50µm was made more porous and undulating prior to the addition of a ~200 µm thick TBC. The blade samples were then thermally aged for 10,000 hours.

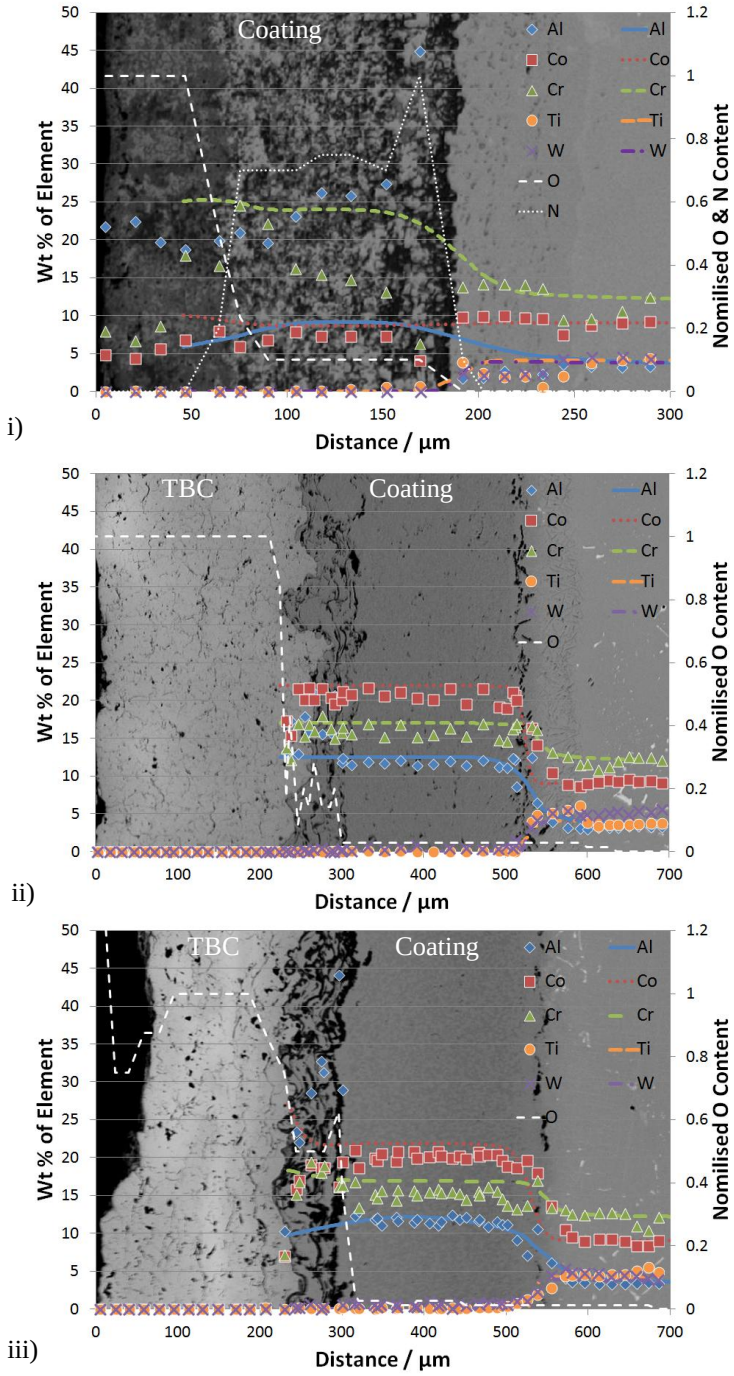

Figure 9. A series of plots for the PWA1483 i) ex-service blade, ii) blade refurbished sample and iii) refurbished sample after 10,000 hours of thermal exposure all showing how the elemental composition of Al, Co, Cr, Ti, W, O for i) ii) and iii) and N for i) vary as function of position. The points and white dashed lines are from measurements taken using EDS in an SEM and the coloured lines on the plots are the predictions from the combined thermodynamic and kinetic calculations. The data are overlaid on a corresponding SEM backscattered detector image.

The coupled thermodynamic and kinetic calculations used the original coating composition but with a thickness of 300 µm and PWA1483 base metal and then a simulated engine age for 27,000 hours. The measured and calculated values are shown in Figure 9 i) and indicate that there is a discrepancy in the Al levels, although the calculated level correlates well with the measured Al levels in the creep samples which had undergone more controlled exposure. The higher measured level in the blade sample may indicate the examined region could be undergoing enhanced degradation. High levels of N were observed in the coating, Figure 9 i), and an absence of S, not shown on figure, which may suggest that the coating has been degraded by high temperature oxidation.

The main measured compositional difference in the coating between the refurbished sample and aged sample is an elevated Al and O content in the first 50 µm of the oxidation coating, as shown in Figure 9 ii) and iii). The phase analysis also showed a significant depletion of the beta phase in the first ~50 µm of the oxidation coating, as shown in Figure 10, while the coupled thermodynamic and kinetic calculations show beta levels not changing as significantly in this region. The calculated Al remains at the as coated level even after simulated thermal exposure for 10,000 hours. This is a similar observation to that made in the simulated refurbishment calculations. The measured composition in the first 50 µm showed relatively higher levels of O compared to the remaining oxidation coating, Figure 9 iii). The coating prior to thermally ageing in the first 50 µm also had higher levels of O compared to the remaining oxidation coating. The application of the coating in this region was more porous and formed of thinner layers, this would increase the surface area and aid diffusion in preference to the remaining oxidation coating. The coupled thermodynamic and kinetic calculations do not currently take the porosity of the coating into account, and the coating is assumed to be homogenous. The beta level could be measured on additional samples which had either been exposed for longer or have seen a high temperature to evaluate if a porous outer layer significantly affects beta depletion.

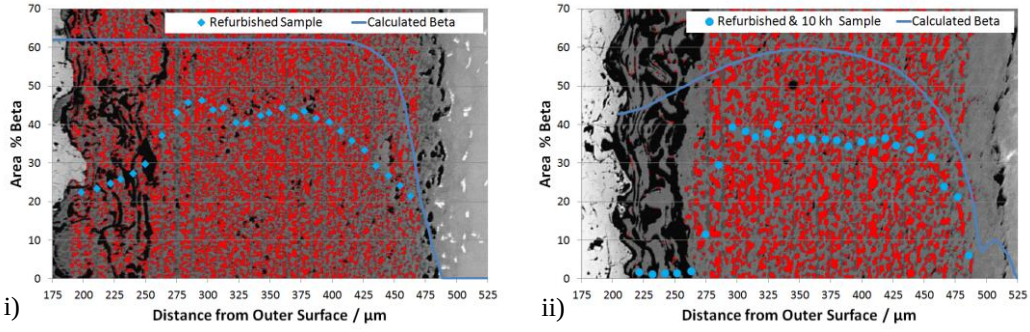

Figure 10. A series of plots for PWA1483 i) initial blade refurbished sample, ii) refurbished sample after 10,000 hours of thermal exposure showing how the amount of beta phase varies through the coating. The points are from measurement and the line is from the coupled thermodynamic and kinetic calculations. The data are overlaid on a corresponding SEM backscattered detector image with red indicating the phase being analysed.

CONCLUSIONS

The work that has been undertaken has shown that using an combination of phase stability predictions, combined thermodynamic and kinetic diffusional calculations, experimental measurements of creep, ex-service blade and heat treated samples using electron imaging, image analysis and chemical mapping techniques it is possible to determine heat treatment windows to alter γ′ morphology and quantify these changes. The initial development of combined

thermodynamic and kinetic calculations to simulate the refurbishment heat treatment and re-coating process have shown generally good agreement with experimental observations, and have been able to highlight where future developments are required.

The main conclusions from this research are:

- The γ′ rafted morphology in PWA1483 can be altered to a cubic form with a size distribution similar to the initial coated sample.
- Thermodynamic equilibrium calculations can be used to aid in the identification of suitable heat treatment windows.
- Coupled thermodynamic and kinetic calculations can give an understanding of coating ageing behaviour.
- The effects of refurbishment of a coating and the base alloy could be initially assessed using coupled thermodynamic and kinetic calculations.

Further Work

Evaluate and optimise the coupled thermodynamic and kinetic on refurbished and retested creep samples when they become available.

ACKNOWLEDGEMENTS

The authors would like to acknowledge the financial support of RWEnpower, Swindon, UK for this research.

REFERENCES

[1] Saunders N. *et al.*, "Computer Modelling of Material Properties", *Materials Design Approaches and Experiences*, ed. J.-C. Zhao et al. (TMS, 2001), 185.

[2] Karunaratne, M. S. A. *et al*., "A Multicomponent Diffusion Model for the Prediction of Microstructural Evolution in Coated Ni-based Superalloy Systems", Materials Science and Technology, 25(2), (2009), pp 287-299.

[3] Davies, R. H. *et al*. "MTDATA -Thermodynamics and Phase Equilibrium Software from the National Physical Laboratory". *CALPHAD.* June 2002, Vol. 26, 2, pp. 229-271.

[4] Saunders, N, "Phase Diagram Calculations for Ni-based Superalloys." [ed.] R. D. Kissinger, *et al*: *The Minerals, Metals & Materials Society*, Warrendale, PA 15086-7528, USA, 1996. Proceedings of the Eighth International Symposium on Superalloys. pp. 101-110.

[5] Meier, S. M., Nissley, D. M. and Sheffler, K. D. "Thermal Barrier Coating Life Prediction Model Development, {Phase II Final Report}". NASA Lewis Research Center, National Aeronautics and Space Administration. 1991. NASA Contractor Report. 18911/NAS3-23944.

[6] Rowe, A. *et al.*, "Microstructural Evolution of Single Crystal and Directionally Solidified Rejuvenated Nickel Superalloys", [ed.] Huron, E. S. *et al., The Minerals, Metals & Materials Society*, Warrendale, PA 15086-7528, USA, 1996. Proceedings of the Twelfth International Symposium on Superalloys. pp. 245-254.